

## Tetrathiafulvalene End-Functionalized Poly(*N*-isopropylacrylamide): A New Class of Amphiphilic Polymer for the Creation of Multistimuli Responsive Micelles

Julien Bigot,<sup>†</sup> Bernadette Charleux,<sup>‡</sup> Graeme Cooke,<sup>\*,§</sup> François Delattre,<sup>||</sup> David Fournier,<sup>†</sup> Joël Lyskawa,<sup>†</sup> Léna Sambe,<sup>†</sup> François Stoffelbach,<sup>⊥</sup> and Patrice Woisel<sup>\*,†</sup>

Univ Lille Nord de France, F-59000 Lille, France USTL, Unité des Matériaux Et Transformations (UMET, UMR 8207), Team "Ingénierie des Systèmes Polymères" (ISP), 59650 Villeneuve d'Ascq Cedex, France, Université de Lyon, Univ. Lyon 1, CPE Lyon, CNRS UMR 5265, Laboratoire de Chimie Catalyse Polymères et Procédés (C2P2), Equipe LCPP Bat 308F, 43 Bd du 11 novembre 1918, F-69616 Villeurbanne, France, Glasgow Centre for Physical Organic Chemistry, WestCHEM, Department of Chemistry, Joseph Black Building, University of Glasgow, Glasgow, U.K., G12 8QQ, U.K., UCEIV (Unité de Chimie Environnementale et Interactions sur le Vivant), EA 4492, Université du Littoral Côte d'Opale, Avenue M. Schumann 59140 Dunkerque, France, and UPMC–CNRS Univ. Paris 6, UMR 7610 Laboratoire de Chimie des Polymères, 4 Place Jussieu, Tour 44–54, 75252 Paris Cedex 05, France

Received April 6, 2010; E-mail: graemec@chem.gla.ac.uk; patrice.woisel@ensc-lille.fr

**Abstract:** In this article, we report the formation of micelles from a tetrathiafulvalene (TTF) end-functionalized poly(*N*-isopropylacrylamide) (poly(NIPAM)) derivative (1). We have determined the critical aggregation concentration (CAC) and average diameter of the micelles using fluorescence spectroscopy and dynamic light scattering experiments, respectively. We have exploited the NIPAM backbone of the polymer to thermally transform the swollen hydrophilic poly(NIPAM) derivative to a more globular hydrophobic state at the lower critical solution temperature (LCST). Finally, we have shown that we can exploit the chemical oxidation and complexation properties of the TTF unit to disrupt the micelle architecture to release the hydrophobic dye Nile Red from the interior of the micelle.

### Introduction

Micelles fabricated from macromolecular species<sup>1</sup> have attracted considerable interest due to their potential roles in a diverse range of applications including drug delivery<sup>2</sup> and catalysis.<sup>3</sup> These nanosized systems are generally fabricated from amphiphilic block copolymers, which spontaneously form micelles through inter- or intramolecular association upon

contact with an aqueous environment. As amphiphilicity<sup>4</sup> plays a major role in the self-assembly processes, much effort has been directed toward engineering "smart" micelle systems from polymers featuring stimuli-responsive hydrophilic/hydrophobic properties. Current approaches toward the development of responsive polymeric micelles have involved the introduction of redox,<sup>5</sup> temperature,<sup>6</sup> pH,<sup>7</sup> photochemical,<sup>8</sup> and enzyme<sup>9</sup> sensitive groups into the polymer backbone. Host–guest

<sup>†</sup> Univ Lille Nord de France.

<sup>‡</sup> Université de Lyon.

<sup>§</sup> Glasgow Centre for Physical Organic Chemistry.

<sup>||</sup> EA2599 Université du Littoral Côte d'Opale.

<sup>⊥</sup> UPMC–CNRS Univ. Paris 6.

- (1) (a) Schatz, C.; Louguet, S.; Le Meins, J.-F.; Lecommandoux, S. *Angew. Chem., Int. Ed.* **2009**, *48*, 2572–2575. (b) Riess, G. *Prog. Polym. Sci.* **2003**, *28*, 1107–1170. (c) McCormick, C. L.; Sumerlin, B. S.; Lokitz, B. S.; Stempka, J. E. *Soft Matter* **2008**, *4*, 1760–1773. (d) Smith, A. E.; Xu, X.; McCormick, C. L. *Prog. Polym. Sci.* **2010**, *35*, 45–93. (e) Lutz, J.-F. *Polym. Int.* **2006**, *55*, 979–993.
- (2) For examples, see: (a) Ganta, S.; Devalapally, H.; Shahiwal, A.; Amiji, M. J. *Controlled Release* **2008**, *126*, 187–204. (b) Kataoka, K.; Harada, A.; Nagasaki, Y. *Adv. Drug Delivery Rev.* **2001**, *47*, 113–131. (c) Rapoport, N. *Prog. Polym. Sci.* **2007**, *32*, 962–990. (d) Meng, F.; Zhong, Z.; Feijen, J. *Biomacromolecules* **2009**, *10*, 197–209. (e) Stenzel, M. H. *Chem. Commun.* **2008**, 3486–3503. (f) Wei, H.; Cheng, S.-X.; Zhang, X.-Z.; Zhuo, R.-X. *Prog. Polym. Sci.* **2009**, *34*, 893–910.
- (3) Vriezema, D. M.; Aragonès, M. C.; Elemans, J. A. A. W.; Cornelissen, J. J. L. M.; Rowan, A. E.; Nolte, R. J. M. *Chem. Rev.* **2005**, *105*, 1445–1490.

- (4) (a) Wang, Y.; Xu, H.; Zhang, X. *Adv. Mater.* **2009**, *21*, 2849–2864. (b) Wang, C.; Guo, Y.; Wang, Y.; Xu, H.; Zhang, X. *Chem. Commun.* **2009**, 5380–5382. (c) Sundararaman, A.; Stephan, T.; Grubbs, R. B. *J. Am. Chem. Soc.* **2008**, *130*, 12264–12265.
- (5) For recent examples, see: (a) Power-Billard, K. N.; Spontak, R. J.; Manners, I. *Angew. Chem., Int. Ed.* **2004**, *43*, 1260–1264. (b) Ma, N.; Li, Y.; Xu, H.; Wang, Z.; Zhang, X. *J. Am. Chem. Soc.* **2010**, *132*, 442–443. (c) Napoli, A.; Valentini, M.; Tirelli, N.; Müller, M.; Hubbell, J. A. *Nat. Mater.* **2004**, *3*, 183–189. (d) Wang, X.; Wang, H.; Coombs, N.; Winnik, M. A.; Manners, I. *J. Am. Chem. Soc.* **2005**, *127*, 8924–8925. (e) Cerritelli, S.; Velluto, D.; Hubbell, J. A. *Biomacromolecules* **2007**, *8*, 1966–1972. (f) Dong, W.-F.; Kishimura, A.; Anraku, Y.; Chuanoi, S.; Kataoka, K. *J. Am. Chem. Soc.* **2009**, *131*, 3804–3805.
- (6) Morishima, Y. *Angew. Chem., Int. Ed.* **2007**, *46*, 1370–1372.
- (7) Klaiherd, A.; Nagamani, C.; Thayumanavan, S. *J. Am. Chem. Soc.* **2009**, *131*, 4830–4838.
- (8) Goodwin, A. P.; Mynar, J. L.; Ma, Y.; Fleming, G. R.; Fréchet, J. M. J. *J. Am. Chem. Soc.* **2005**, *127*, 9952–9953.
- (9) Amir, R. J.; Zhong, S.; Pochan, D. J.; Hawker, C. J. *J. Am. Chem. Soc.* **2009**, *131*, 13949–13951.

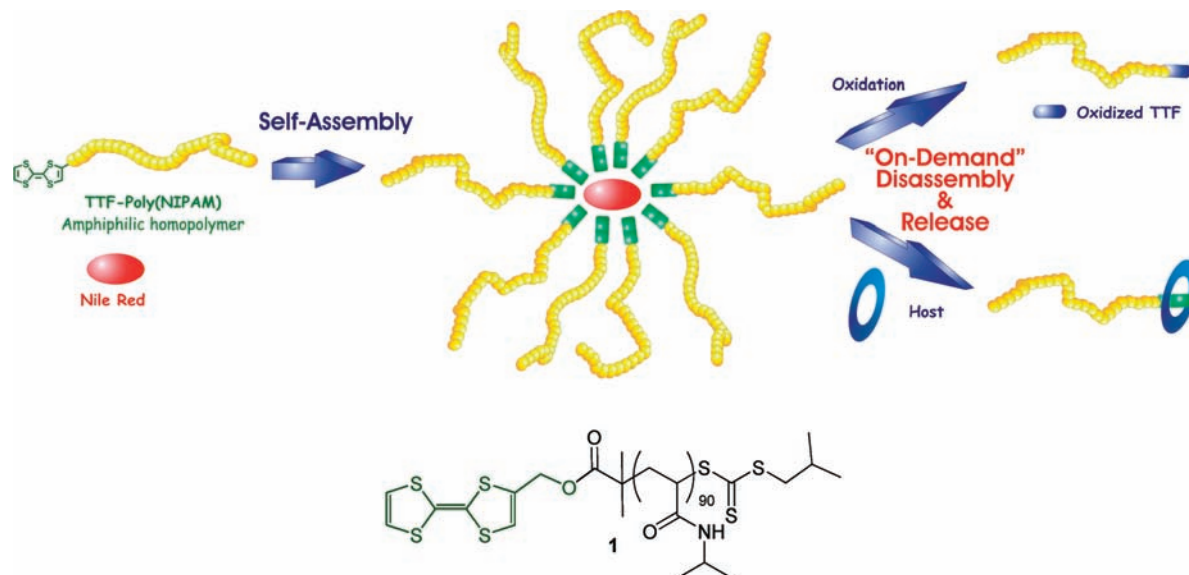


**Figure 1.** Schematic representation of the formation of micelles from polymer **1** and their subsequent disassembly.

interactions have also been employed to control the self-assembly of polymer-based micelles.<sup>10</sup>

Tetrathiafulvalene (TTF) due to its easily accessed oxidized states (TTF<sup>+</sup> and TTF<sup>2+</sup>) and rich synthetic chemistry, has undoubtedly become one of the most studied redox active organic materials.<sup>11</sup> Traditionally, the main applications of TTF have focused upon its incorporation as a  $\pi$ -electron donor moiety in conducting charge-transfer complexes.<sup>12</sup> More recently, in view of the disparate physical properties displayed by TTF in its different redox states,<sup>13</sup> these units have been utilized in a range of applications including the fabrication of redox-controllable: molecular machines,<sup>14</sup> biological probes,<sup>15</sup> switches,<sup>16</sup> logic gates,<sup>17</sup> liquid crystals,<sup>18</sup> and gels.<sup>19</sup>

Herein, we report the successful engineering of novel “smart” polymeric core–shell nanospheres resulting from an amphiphilic linear TTF end-functionalized poly(*N*-isopropylacrylamide) (poly(NIPAM)) homopolymer (**1**). In this system, we anticipate that the TTF<sup>20</sup> unit and a poly(NIPAM) segment act as hydrophobic and hydrophilic moieties, respectively. We have shown that polymer **1** can self-assemble in water affording polymeric micelles that are able to respond to multiple stimuli including: temperature, redox processes, and host–guest interactions (Figure 1). In particular, we have demonstrated that the chemical oxidation of the TTF moiety to its TTF<sup>2+</sup> state results in a disruption of the micelle architecture, presumably by rendering the inner core more hydrophilic. In addition, we report the use of the tetracationic macrocycle cyclobis(paraquat-*p*-phenylene) (CBPQT<sup>4+</sup>, 4Cl<sup>−</sup>) as a powerful material to disrupt

micelles by complexation with the TTF unit of **1**. As a proof of concept, we also report the impact of both stimuli on the release of Nile Red (NR) from the micelle core.

## Results and Discussion

The TTF-functionalized polymer **1** ( $M_n = 9730$  g/mol, PDI = 1.14) was synthesized following our previously reported

- (10) For representative recent examples, see: (a) Chen, Y.; Dong, C.-M. *J. Phys. Chem. B* **2010**, *114*, 7461–7468. (b) Chen, Y.; Pang, X. H.; Dong, C. M. *Adv. Funct. Mater.* **2010**, *20*, 579–586. (c) Liu, H.; Zhang, Y.; Hu, J.; Li, C.; Liu, S. *Macromol. Chem. Phys.* **2009**, *210*, 2125–2137. (d) Ren, S.; Chen, D.; Jiang, M. *J. Polym. Sci., Polym. Chem.* **2009**, *47*, 4267–4278. (e) Huang, J.; Ren, L.; Chen, Y. *Polym. Int.* **2008**, *57*, 714–721. (f) Zhang, J.; Ma, P. X. *Angew. Chem., Int. Ed.* **2009**, *48*, 964–968. (g) Chipper, M.; Winter, A.; Hoogenboom, R.; Egbe, D. A. M.; Wouters, D.; Hoepfener, S.; Fustin, C.-A.; Gohy, J.-F.; Schubert, U. S. *Macromolecules* **2008**, *41*, 8823–8831.
- (11) *TTF Chemistry. Fundamentals and Applications of Tetrathiafulvalene*; Yamada, J., Sugimoto, T., Eds.; Springer Verlag: Heidelberg, 2004.
- (12) Bryce, M. R. *Chem. Soc. Rev.* **1991**, *20*, 355–390.
- (13) For a recent review, see: Canevet, D.; Sallé, M.; Zhang, G.; Zhang, D.; Zhu, D. *Chem. Commun.* **2009**, 2245–2269.

- (14) For representative recent examples, see: (a) Ashton, P. R.; Balzani, V.; Becher, J.; Credi, A.; Fyfe, M. C. T.; Mattersteig, G.; Menzer, S.; Nielsen, M. B.; Raymo, F. M.; Stoddart, J. F.; Venturi, M.; White, A. J. P.; Williams, D. J. *J. Am. Chem. Soc.* **1999**, *121*, 3951–3957. (b) Devonport, W.; Blower, M. A.; Bryce, M. R.; Goldenberg, L. M. *J. Org. Chem.* **1997**, *62*, 885–887. (c) Balzani, V.; Credi, A.; Mattersteig, G.; Matthews, O. A.; Raymo, F. M.; Stoddart, J. F.; Venturi, F.; White, A. J. P.; Williams, D. J. *J. Org. Chem.* **2000**, *65*, 1924–1936. (d) Asakawa, M.; Ashton, P. R.; Balzani, V.; Credi, A.; Mattersteig, G.; Matthews, M.; Montali, O. A.; Spencer, N.; Stoddart, J. F.; Venturi, M. *Chem.—Eur. J.* **1997**, *3*, 1992–1996. (e) Zhao, Y. L.; Dichtel, W. R.; Trabolsi, A.; Saha, S.; Aprahamian, I.; Stoddart, J. F. *J. Am. Chem. Soc.* **2008**, *130*, 11294–11296. (f) Asakawa, M.; Ashton, P. R.; Balzani, V.; Credi, A.; Hamers, C.; Mattersteig, G.; Montalti, M.; Shipway, A. N.; Spencer, N.; Stoddart, J. F.; Tolley, M. S.; Venturi, M.; White, A. J. P.; Williams, D. J. *Angew. Chem., Int. Ed.* **1998**, *37*, 333–337.
- (15) Li, X.; Zhang, G.; Ma, H.; Zhang, D.; Li, J.; Zhu, D. *J. Am. Chem. Soc.* **2004**, *126*, 11543–11548.
- (16) Zhou, Y.; Zhang, D.; Zhu, L.; Shuai, Z.; Zhu, D. *J. Org. Chem.* **2006**, *71*, 2123–2130.
- (17) Zhou, Y.; Wu, H.; Qu, L.; Zhang, D.; Zhu, D. *J. Phys. Chem. B* **2006**, *110*, 15676–15679.
- (18) Yasuda, T.; Tanabe, K.; Tsuji, T.; Cotí, K. K.; Aprahamian, I.; Stoddart, J. F.; Kato, T. *Chem. Commun.* **2010**, *46*, 1224–1226.
- (19) For examples see: (a) Wang, C.; Zhang, D.; Zhu, D. *J. Am. Chem. Soc.* **2005**, *127*, 16372–16373. (b) Kitahara, T.; Shirakawa, M.; Kawano, S.; Beginn, U.; Fujita, N.; Shinkai, S. *J. Am. Chem. Soc.* **2005**, *127*, 14980–14981. (c) Puigmart-Luis, J.; Laukhin, V.; del Pino, A. P.; Vidal-Gancedo, J.; Rovira, C.; Laukhina, E.; Amabilino, D. B. *Angew. Chem., Int. Ed.* **2007**, *46*, 238–241. (d) Zhao, Y. L.; Aprahamian, I.; Trabolsi, A.; Erina, N.; Stoddart, J. F. *J. Am. Chem. Soc.* **2008**, *130*, 6348–6350.
- (20) For examples of micelles including TTF units, see: (a) Eddowes, M. J.; Grätzel, M. *J. Electroanal. Chem.* **1983**, *152*, 143–155. (b) Leheny, A. R.; Rossetti, R.; Brus, L. E. *J. Phys. Chem.* **1985**, *89*, 4091–4093. (c) Georges, J.; Desmetre, S. *J. Colloid Interface Sci.* **1987**, *118*, 192–200. (d) Georges, J.; Desmetre, S. *J. Electrochim. Acta* **1986**, *31*, 1519–1524. (e) Eddowes, M. J.; Grätzel, M. *J. Electroanal. Chem.* **1984**, *163*, 31–64. (f) Grätzel, C. K.; Grätzel, M. *J. Phys. Chem.* **1982**, *86*, 2710–2714.

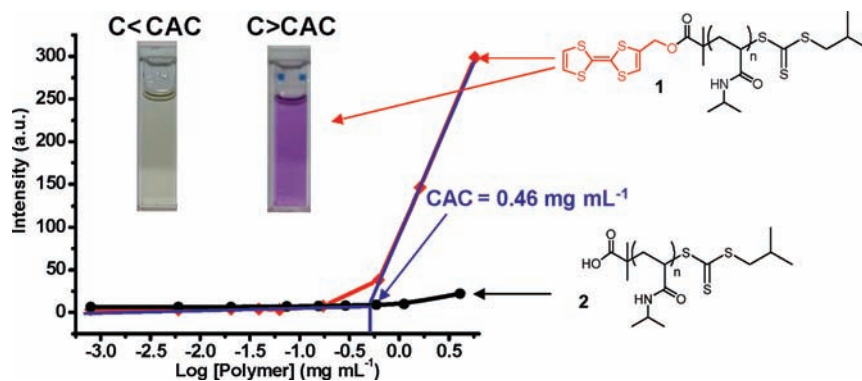


**Figure 2.** Intensity of the emission fluorescence spectra of NR as a function of the logarithm of the concentration of **1** (red line) and **2** (black line).  $\lambda_{\text{ex}} = 530$  nm.  $\lambda_{\text{em}} = 625$  nm. Recorded at 24 °C.

procedure by reversible addition–fragmentation chain transfer (RAFT) polymerization.<sup>21</sup> The neutral  $\omega$ -isobutyl fragment was incorporated into the polymer due to its ability to mimic the structure of the NIPAM repeat unit.<sup>22</sup> Self-assembly of **1** was induced via direct dissolution in water, and the dilute aqueous solution properties were assessed using fluorescence spectroscopy, dynamic light scattering (DLS), and cryogenic transmission electron microscopy (cryo-TEM). The formation of a polymeric micelle assembly was initially investigated by fluorescence spectroscopy. The dye NR, due to its strong hydrophobicity, has very poor solubility in aqueous media, and it displays a low fluorescence emission below the critical aggregation concentration (CAC) of micelles. However, upon micellization, NR can be encapsulated inside the hydrophobic microenvironment of the core–shell structure, thereby inducing a sharp increase of the fluorescence emission intensity of this compound.<sup>7</sup> The dependence of the relative fluorescence intensity of NR versus the logarithm of the concentration of **1** and of poly(NIPAM) **2** ( $M_n = 8100$  g/mol, PDI = 1.13) is presented in Figure 2. While an abrupt increase in emission intensity of NR was observed for **1** at a concentration of about 0.46 mg/mL suggesting the onset of micelle formation and the transfer of NR into the hydrophobic core of the micelle, no significant change in the fluorescence intensity of NR was observed when similar experiments were undertaken using polymer **2**. These results suggest that the TTF unit plays an important role in the micellization process of **1**, presumably a consequence of its hydrophobic character and ability to participate in intermolecular  $\pi$ – $\pi$  stacking and S $\cdots$ S interactions within the micelle architecture.<sup>23</sup>

To obtain further evidence of the self-assembly of **1**, DLS experiments were carried out which revealed the existence of a monomodal size distribution for the micelles (average micelle diameter = 26 nm) (Figure 3A). Furthermore, poly(NIPAM) **2**, which does not bear a TTF moiety, had a significantly smaller diameter (<10 nm) suggesting that no aggregation occurred, thereby further indicating the important role played by the TTF unit in the self-assembly process of **1**. Cryo-TEM was also used for the direct visualization of the size and morphology of the micelles of **1**. As depicted in Figure 3B, cryo-TEM shows that individual spherical micelles are obtained for **1** and that the size of the micellar core

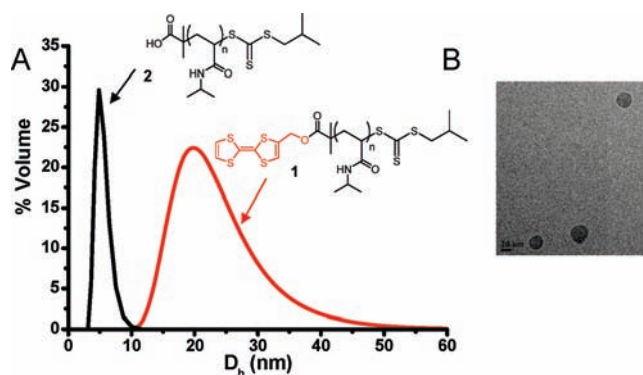


**Figure 3.** (A) DLS data for **1** and **2** recorded at 24 °C and at a concentration of 3 mg mL<sup>-1</sup> and (B) cryo-TEM image for micelles obtained from **1**.

( $D \approx 29$  nm, measured from the images) correlates well with the mean hydrodynamic diameter obtained by DLS.

As described above, poly(NIPAM) was selected for the polymeric backbone for its hydrophilic properties to promote the self-assembly of **1** to form micelles. Moreover, it is well established that polymers of this type can possess thermoresponsive properties. Indeed, it has been shown that temperature-responsive polymers such as poly(NIPAM) undergo sharp coil (hydrophilic) to globule (hydrophobic) transitions in water that lead to phase separation at the lower critical solution temperature (LCST).<sup>24</sup> Thus, in our micellar system, if the hydrophilic poly(NIPAM) outer shell is converted to a more hydrophobic state in response to changing temperature, the amphiphilicity of micelles will be altered, resulting in the formation of a more hydrophobic polymer. To investigate the possible LCST behavior of **1**, a solution of this polymer in water was heated to 40 °C. As expected, the transparent solution at ambient temperature underwent an abrupt change in turbidity when the temperature reached the LCST of the polymer (Figure 4A), due to the hydrophilic to hydrophobic change in the polymer structure. The transmittance and the hydrodynamic diameter (Figure 4B) of **1** as a function of temperature was examined to determine the actual LCST. A cloud point of approximately 30.5 °C was obtained, which is consistent with typical LCST values of poly(NIPAM) derivatives ( $\sim 32$  °C).<sup>24b</sup> Indeed, in our polymeric micelles, we expect that hydrophobic TTF moieties are sequestered

(21) Bigot, J.; Charleux, B.; Cooke, G.; Delattre, F.; Fournier, D.; Lyskawa, J.; Stoffelbach, F.; Woisel, P. *Macromolecules* **2010**, *43*, 82–90.  
 (22) Kujawa, P.; Segui, F.; Shaban, S.; Diab, C.; Okada, Y.; Tanaka, F.; Winnik, F. M. *Macromolecules* **2006**, *39*, 341–348.  
 (23) Zhang, K.-D.; Wang, G. T.; Zhao, X.; Jiang, X.-K.; Li, Z. -T. *Langmuir* **2010**, *26*, 6878–6882.

(24) (a) Schild, H. G. *Prog. Polym. Sci.* **1992**, *17*, 163–249. (b) Barker, I. C.; Cowie, J. M. G.; Huckerby, T. N.; Shaw, D. A.; Soutar, I.; Swanson, L. *Macromolecules* **2003**, *36*, 7765–7770. (c) Winnik, F. M. *Macromolecules* **1990**, *23*, 233–242. (d) Ringsdorf, H.; Simon, J.; Winnik, F. M. *Macromolecules* **1992**, *25*, 7306–7312. (e) Rimmer, S.; Soutar, I.; Swanson, L. *Polym. Int.* **2009**, *58*, 273–278.

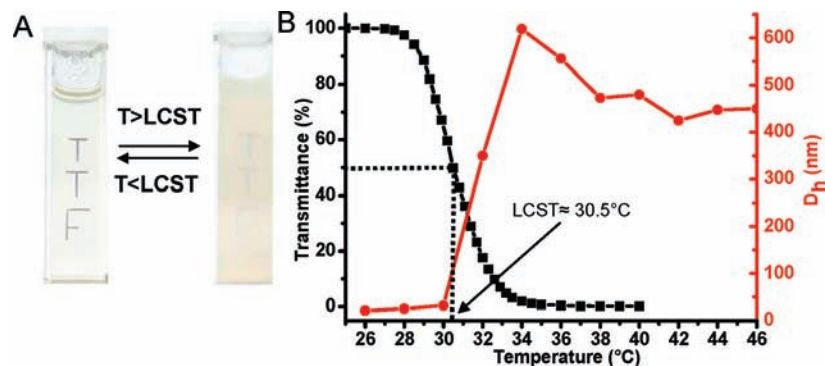


**Figure 4.** (A) Photograph showing an aqueous solution of **1** at room temperature (left) and at 40 °C (right). (B) Transmittance (black line) and hydrodynamic diameter (red line) vs temperature for **1** (3 mg mL<sup>-1</sup>) in aqueous solution.

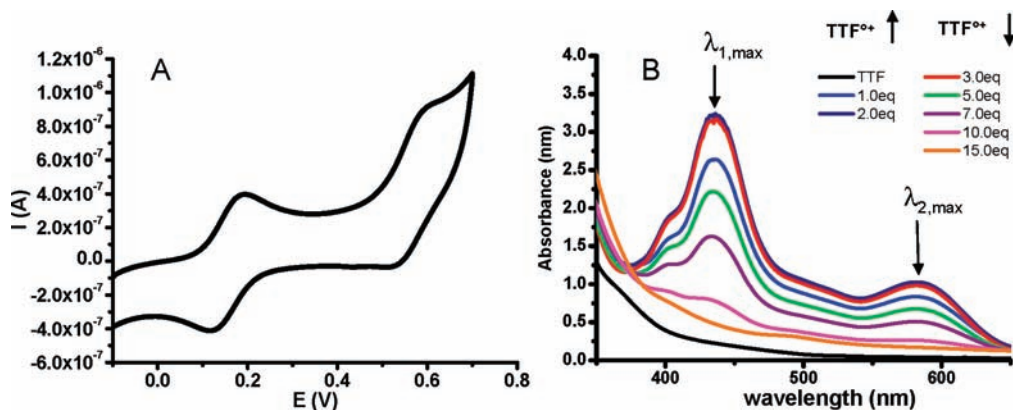


**Figure 5.** (A) Cyclic voltammety of **1** (1 mM) in 0.1 M NaCl/H<sub>2</sub>O at a scan rate = 100 mV s<sup>-1</sup>. Recorded at 12 °C. (B) UV-vis titration changes of **1** (1 mM) upon addition of Fe(ClO<sub>4</sub>)<sub>3</sub>. Recorded at 20 °C.

in the inner core and isolated from the aqueous media and, therefore, do not influence the LCST of the poly(NIPAM) outer shell significantly. DLS measurements (Figure 4B) showed that above the LCST (44 °C) the polymer tends to form larger aggregates displaying a mean diameter of  $D_h \approx 450$  nm.<sup>1b</sup>

We have also exploited the ability of the hydrophobic TTF unit to be oxidized into its more hydrophilic TTF<sup>2+</sup> dicationic state to modify the amphiphilicity of the polymer and thus micelle stability.<sup>25</sup> First, we demonstrated that **1** was able to form the TTF<sup>2+</sup> in aqueous solution by using cyclic voltammety (CV). To this end, CV of **1** was recorded at 12 °C, a temperature which is below its LCST (16 °C in NaCl 0.1 M) to avoid precipitation (see Supporting Information). Furthermore, DLS and fluorescence measurements indicated that under these conditions micelles were not present (see Supporting Information). Polymer **1** gives rise to two reversible one-electron oxidation waves at +0.17 and +0.48 V corresponding to the two-step oxidation (TTF → TTF<sup>•+</sup> → TTF<sup>2+</sup>) of the TTF unit (Figure 5A). Next, the influence the chemical oxidation of the TTF unit at the terminus of the polymer to the TTF<sup>2+</sup> state has on the size and morphology of the micelles was investigated. To this end, Fe(ClO<sub>4</sub>)<sub>3</sub> was employed as an oxidizing agent to produce the TTF<sup>2+</sup> state. The formation of the TTF<sup>2+</sup> was monitored by UV-vis spectroscopy.<sup>14c</sup> The addition, at 20 °C, of one equivalent

of Fe(ClO<sub>4</sub>)<sub>3</sub> to a solution of **1** resulted in the appearance of the two characteristic absorption bands of the TTF<sup>•+</sup> species ( $\lambda_1 = 445$  nm,  $\lambda_2 = 590$  nm) which progressively decrease following the addition of more than 2 equiv of Fe(ClO<sub>4</sub>)<sub>3</sub>, thereby suggesting the transformation of the TTF<sup>•+</sup> into the TTF<sup>2+</sup> unit (Figure 5B). These experiments indicated that ~15 equiv of Fe(ClO<sub>4</sub>)<sub>3</sub> was required to fully oxidize the TTF unit, suggesting that this moiety is buried in the inner hydrophobic core and therefore not easily accessible to Fe(ClO<sub>4</sub>)<sub>3</sub>.

Next, the influence of the formation of the TTF<sup>2+</sup> unit at the terminus of the polymer on the size and morphology of the micelles was investigated by cryo-TEM. A cryo-TEM image was recorded upon the addition of an excess of Fe(ClO<sub>4</sub>)<sub>3</sub> (Figure 6A), which clearly revealed the presence of smaller ill-defined asymmetrical aggregates (<10 nm) upon complete oxidation of the TTF unit. The ability of the micelles to release

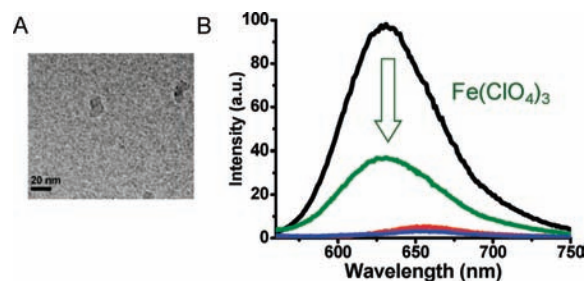


**Figure 6.** (A) Cryo-TEM image of **1** (3 mg mL<sup>-1</sup>) in the presence of Fe(ClO<sub>4</sub>)<sub>3</sub> (18 equiv). (B) Fluorescence spectra of NR (red line), NR + 18 equiv of Fe(ClO<sub>4</sub>)<sub>3</sub> (blue line), NR + **1** (black line), and NR + **1** + 18 equiv of Fe(ClO<sub>4</sub>)<sub>3</sub> (green line). Recorded at 20 °C.

(25) For examples of redox-active ferrocene-functionalized poly(NIPAM) derivatives, see: (a) Zuo, F.; Luo, C.; Ding, X.; Zheng, Z.; Cheng, X.; Peng, Y. *Supramol. Chem.* **2008**, *20*, 559–564. (b) Kuramoto, N.; Shishido, Y. *Polymer* **1998**, *39*, 669–675. (c) Fu, H.; Policarpio, D. M.; Batteas, J. D.; Bergbreiter, D. E. *Polym. Chem.* **2010**, *1*, 631–633. (d) Feng, C.; Shen, Z.; Yang, L.; Hu, J.; Lu, G.; Huang, X. *J. Polym. Sci., Polym. Chem.* **2009**, *47*, 4346–4357.

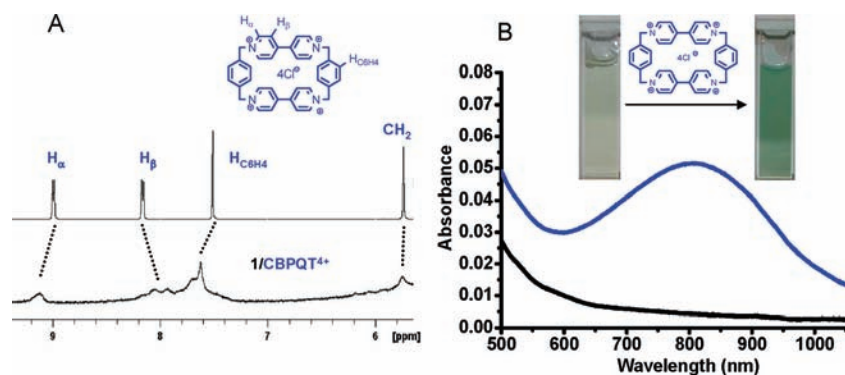


**Figure 7.** (A) Partial  $^1\text{H}$  NMR spectra of  $\text{CBPQT}^{4+}$ ,  $4\text{Cl}^-$  (top) and  $\text{CBPQT}^{4+}$ ,  $4\text{Cl}^-/1$  (1/1 molar ratio) (bottom) in  $\text{D}_2\text{O}$ . Recorded at  $20^\circ\text{C}$ . (B) UV-vis spectra of **1** (black line) ( $3\text{ mg mL}^{-1}$ ) in  $\text{H}_2\text{O}$  and in the presence of  $\text{CBPQT}^{4+}$  (blue line) ( $3\text{ mg mL}^{-1}$ ). Recorded at  $20^\circ\text{C}$ .

an encapsulated hydrophobic molecule by oxidizing the TTF unit was next investigated. As shown in Figure 6B, the location of NR in the micelle core induces a spectral blue shift (30 nm) reflecting the presence of NR in a hydrophobic environment. The addition of  $\text{Fe}(\text{ClO}_4)_3$  to a solution of the micelles resulted in a dramatic decrease in the fluorescence intensity of NR, thereby indicating the partial release ( $\sim 65\%$ ) of the NR from the micelle environment. This result is consistent with the cryo-TEM data which show the formation of smaller aggregates upon addition of the oxidizing agent. DLS and fluorescence control experiments were carried out with polymer **1** in the presence of 54 equiv of  $\text{NaClO}_4$  (see Supporting Information). These investigations revealed that the micelle architecture persists and that no significant variation of the fluorescence intensity of the encapsulated NR occurred, respectively, thereby indicating that micelle disruption was not merely due to salt effects and that oxidation by  $\text{Fe}^{3+}$  plays a key role in the disruption of the micelles.<sup>26</sup>

It is well-established that the TTF moiety is able to form complexes with  $\pi$ -electron-deficient systems such as  $\text{CBPQT}^{4+}$ . In particular, complexes fabricated from  $\text{CBPQT}^{4+}$  and TTF units have become important building blocks for the development of redox tunable supramolecular complexes.<sup>14a,b</sup> Here we have exploited the propensity of the  $\text{CBPQT}^{4+}$  to form complexes with TTF derivatives to modulate the hydrophobicity of the TTF moiety of **1**, thereby leading to the disassembly of the micelle architecture. Complexation between the cyclophane and polymer **1** was investigated using  $^1\text{H}$  NMR spectroscopy. Addition of aliquots of  $\text{CBPQT}^{4+}$  to a solution containing **1** immediately resulted in a significant broadening and change in chemical shift of the  $\text{CBPQT}^{4+}$  proton resonances characteristic of TTF- $\text{CBPQT}^{4+}$ -based complexes of this type (Figure 7A).<sup>21</sup> Furthermore, the addition of aliquots of  $\text{CBPQT}^{4+}$  to a solution containing **1** immediately resulted in the appearance of a green ( $\lambda = 800\text{ nm}$ ) solution that is characteristic of TTF- $\text{CBPQT}^{4+}$  complexes (Figure 7B).<sup>14a,b</sup> The binding between **1** and the  $\text{CBPQT}^{4+}$  was also investigated using isothermal titration calorimetry (ITC) (see Supporting Information). These experiments indicate that addition of the  $\text{CBPQT}^{4+}$  to a solution of **1** in water gives rise to a large association constant  $K_a = 1.7 \pm 0.3 \times 10^6\text{ M}^{-1}$  ( $\Delta H = -16.5\text{ kcal mol}^{-1}$ ). Thus, the  $^1\text{H}$  NMR,

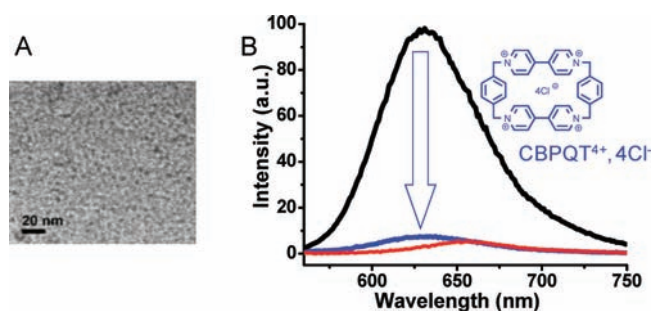


**Figure 8.** (A) Cryo-TEM image of **1** ( $3\text{ mg mL}^{-1}$ ) in the presence of  $\text{CBPQT}^{4+}$  (2 equiv). (B) Fluorescence spectra of NR (red line), NR + **1** (black line), and NR + **1** + 2 equiv of  $\text{CBPQT}^{4+}$  (blue line). Recorded at  $20^\circ\text{C}$ .

UV-vis, and ITC data are consistent with complex formation between the TTF unit of **1** and  $\text{CBPQT}^{4+}$ . Interestingly, when UV-vis and  $^1\text{H}$  NMR experiments were recorded for polymer **1** upon addition of aliquots of dibenzyl viologen ( $2\text{Cl}^-$ ) (DBV), no evidence of complexation was observed (see Supporting Information). Furthermore, the fluorescence spectra of NR encapsulated within micelles of **1** did not change upon addition of aliquots of DBV, suggesting this heterocycle does not induce micelle disruption. Thus, these control experiments indicate the importance of the cyclic structure of  $\text{CBPQT}^{4+}$  to promote effective complexation and subsequent micelle disruption.

We next turned our attention to whether micelles could be disassembled upon complexation with  $\text{CBPQT}^{4+}$ . Cryo-TEM images were recorded for **1** in the presence of the  $\text{CBPQT}^{4+}$ , and a typical result is presented in Figure 8A. This technique clearly demonstrated that a complete micelle disassembly occurred upon the addition of  $\text{CBPQT}^{4+}$ . Furthermore, the release of NR from micelles of **1** was monitored by measuring the fluorescence intensity of NR upon the addition of the  $\text{CBPQT}^{4+}$  (Figure 8B). Interestingly, an almost complete disappearance of the fluorescence intensity of NR was observed, indicating an efficient release of NR occurred upon the addition of  $\text{CBPQT}^{4+}$ . Fluorescence and NMR control experiments indicated that no significant interactions occur between NR and  $\text{CBPQT}^{4+}$  (Supporting Information), thereby suggesting that the change in fluorescence intensity of NR is due to its release from the disassembled micelle upon complexation between **1** and  $\text{CBPQT}^{4+}$ . This complexation-driven disruption of the micelle is presumably due to an increase in the hydrophilic nature of

(26) (a) Zhu, Z.; Sukhishvili, S. A. *Nano* **2009**, *3*, 3595–3605. (b) Zhang, Y.; Furryk, S.; Bergbreiter, D. E.; Cremer, P. S. *J. Am. Chem. Soc.* **2005**, *127*, 14505–14510. (c) Suwa, K.; Yamamoto, K.; Akashi, M.; Takano, K.; Tanaka, N.; Kunugi, S. *Colloid Polym. Sci.* **1998**, *276*, 529–533. (d) Yoshida, E. *Colloid Polym. Sci.* **2009**, *287*, 1365–1368. (e) Liu, X.-M.; Wang, L. S.; Wang, L.; Huang, J.; He, C. *Biomaterials* **2004**, *25*, 5659–5666.

the TTF moiety upon complexation with the tetracationic CBPQT<sup>4+</sup> unit.

### Conclusions

In conclusion, we have designed and synthesized an amphiphilic polymer featuring a redox active TTF hydrophobic unit and a temperature-sensitive hydrophilic poly(NIPAM) shell. This amphiphilic polymer self-associates to form micelles in aqueous media and is able to encapsulate the hydrophobic guest NR. Increasing temperature above the LCST causes the micelles to form large aggregates due to the coil–globule transition of the poly(NIPAM) chains. We have shown that micelles can be disassembled following the chemical oxidation of the TTF moiety to a more hydrophilic dicationic state, thereby inducing the partial release of NR. In addition, we have shown that hydrophilic macrocycle CBPQT<sup>4+</sup> has the ability to complex

with the TTF moiety of **1** leading to a near-complete disruption of the micelle and the efficient release of NR. This methodology paves the way for the formation of a new class of responsive micelles with advanced materials and drug delivery applications.

**Acknowledgment.** P.W. and G.C. thank the Agence Nationale de la Recherche (ANR-09-JCJC-0032-01) and the EPSRC for funding, respectively. The authors are especially grateful to Dr. Eric Larquet (Institut de Minéralogie et de Physique des Milieux Condensés (IMPMC), UMR 7590, C’Nano IdF), for the cryo-TEM analyses.

**Supporting Information Available:** Experimental details indicated in the manuscript. This material is available free of charge via the Internet at <http://pubs.acs.org>.

JA1027452